

Cosmic Origins Spectrograph FUV Grating Performance

Steve Osterman^a, Erik Wilkinson^a, James C. Green^a, Kevin Redman^b

^aCenter for Astrophysics and Space Astronomy, University of Colorado,
Campus box 389, Boulder CO 80309

^bMantech Systems Engineering Corp, Goddard Space Flight Center,
Greenbelt MD 20771

ABSTRACT

The Cosmic Origins Spectrograph (COS) will be the most sensitive UV spectrograph to be flown aboard the Hubble Space Telescope. The COS FUV and NUV channels will provide high sensitivity at resolution greater than 20000 over wavelengths ranging from 115nm to 320nm. We present a brief review of the instrument design, results from the optical testing of FUV gratings and predicted on orbit performance.

Keywords: Hubble Space Telescope, Far Ultraviolet, Spectroscopy, Optical Testing

1. THE COSMIC ORIGINS SPECTROGRAPH: INSTRUMENT OVERVIEW

The Cosmic Origins Spectrograph (COS) will be a high throughput FUV/NUV spectrograph optimized for observing faint, compact objects and will be installed aboard the Hubble Space Telescope in 2004 as part of servicing mission 4. By optimizing the spectrograph for high efficiency observations of faint, compact UV sources, the COS instrument will achieve unprecedented observation efficiencies^{1,2}.

The COS instrument is describe in detail in reference 2, and is briefly reviewed here. COS has two channels: a far ultraviolet (1150-1775Å) and a near ultraviolet channel (1750-3200Å), with each channel further divided into several observing modes by two optics select mechanisms. Light enters the instrument through the 2.5 arc second Primary Science Aperture located on the HST focal surface. This aperture is intentionally oversized and transmits 100% of the aberrated light from a point source. Light from the entrance aperture then falls on one of the three aspheric FUV gratings for observations in the FUV band, or on an aspheric mirror which directs light into the NUV channel.

The FUV channel is a modified Rowland circle spectrograph with one reflection between the entrance aperture and the detector and three FUV gratings mounted on an optics select mechanism. Each grating is recorded onto an aspheric concave surface designed to compensate for spherical aberration while the holographically generated rulings provide astigmatism correction in addition to dispersing the light. Light diffracted from the selected grating then falls onto a crossed delay line microchannel plate detector with an opaque CsI photocathode.³ The combination of a single reflection, outstanding grating and detector performance, and strict maintenance of the optical coatings and detector photocathode, combine to give the instrument its exceptionally high throughput.

The NUV channel employs a Czerny-Turner design with four flat gratings and a flat mirror on an optics select mechanism. Light diffracted from the selected NUV grating falls onto a set of three camera optics and is then focussed onto a MAMA microchannel plate detector with a CsTe photocathode. COS spectroscopic modes are summarized in table 1.

Table 1: COS Spectrographic Modes

Grating	Channel	Wavelength Range	Pass Band per exposure	Required Resolution $\lambda/\Delta\lambda$
G130M	FUV	1150-1450Å	300 Å	20,000-24,000
G160M	FUV	1405-1775Å	370 Å	20,000-24,000
G140L	FUV	1230-2050Å	>820 Å	2500-3500
G185M	NUV	1700-2000Å	3×28Å	20,000-24,000
G225M	NUV	2000-2500Å	3×35Å	20,000-24,000
G285M	NUV	2500-3200Å	3×41Å	20,000-24,000
G230L	NUV	1700-3200Å	1 or 2×400Å	1550-2900

2. FUV GRATING REQUIREMENTS AND DESCRIPTION

All of the FUV gratings have been holographically ruled by Jobin-Yvon on an aspheric fused silica substrate manufactured by the SVG-Tinsly Corporation. The one exception is the G140L Blazed grating, which is under development at J-Y.

The G130M and G160M gratings have an ion etched triangular groove profile with the blaze function providing the maximum groove efficiency within 100Å of the center of the grating's pass band. The G140L gratings have a laminar profile, with a triangular blaze to be attempted in the near future. The minimum acceptable groove efficiency for any wavelength in a grating's passband is 45% for G130M and G160M and 30% for G140L.

The ruled gratings were then transferred to the Goddard Optical Materials and Thin Film Laboratory to receive a MgF₂ protected aluminum coating optimized for 1216Å. Finally, the gratings were bonded to a mounting bezel at Ball Aerospace and tested at the CASA EUV/FUV test facility in Boulder, CO. Reflectivity and groove efficiency requirements are summarized in table 2. Currently, testing on all gratings except for G160M-C has been completed, with a grating from each class exceeding flight requirements.

Table 2: FUV Grating Requirements

Grating	Blaze Efficiency	Coating Reflectivity			
		1150Å	1216Å	1608Å	2000Å
G130M	0.45	0.60	0.82	0.78	0.80
G160M	0.45	0.60	0.82	0.78	0.80
G140L	0.30	0.60	0.82	0.78	0.80

3. FUV GRATING PERFORMANCE VERIFICATION PLAN AND RESULTS

The CASA EUV/FUV test facilities include a 3.0 meter diameter vacuum chamber with a vibration isolated 1.5×3 meter optics bench. The chamber opens into a class 1000 clean room facility where the bench can be removed to for initial setup and alignment. Testing at CASA was intended to verify performance of the gratings and to select the more efficient of the two gratings of each type delivered for use in the COS instrument (assuming both meet the minimum requirements). The tests and success criteria are and procedures are summarized in reference 4 and in the released grating test plans and calibration results⁵, but are reviewed here for convenience. The optical setups are illustrated in figure 1, and discussed below.

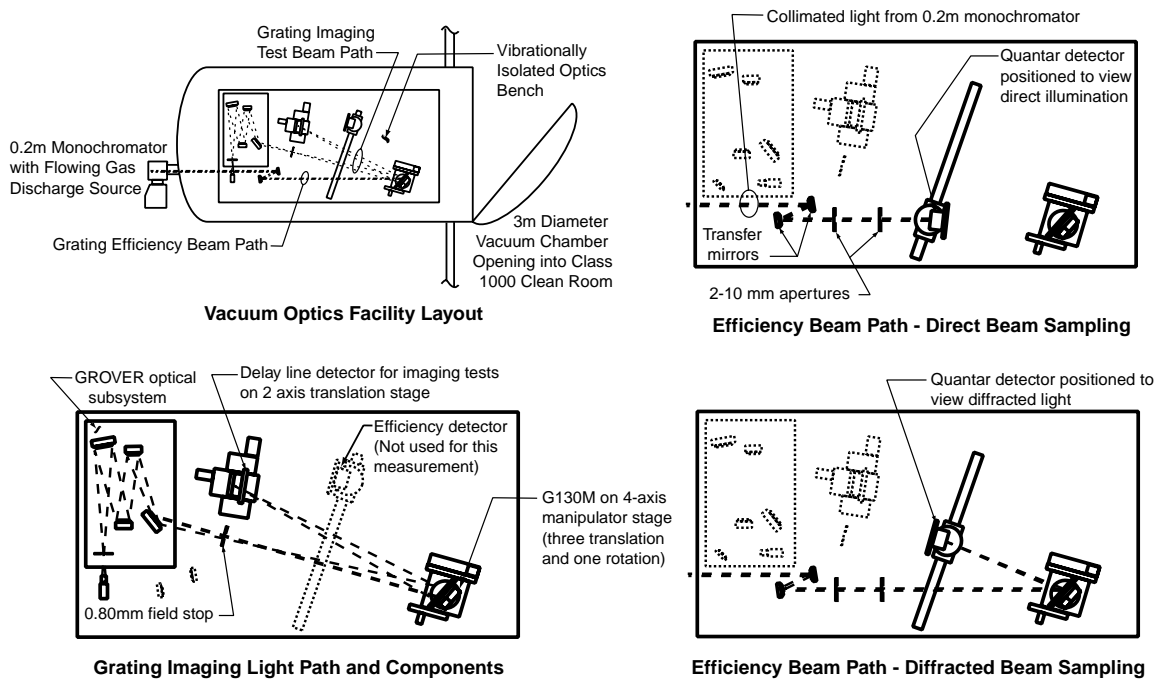


Figure 1: Grating resolution and efficiency test setups

3.1. FUV Imaging and Resolution Tests

The FUV gratings are designed to correct for the HST aberration. Consequently, it is necessary to illuminate the gratings with a UV light source which precisely matches the aberration content and input angle corresponding to the HST field point at the COS entrance aperture in order to accurately assess the grating imaging and dispersion characteristics. This is accomplished by using the Grating Optical Verification Equipment-Reflective (GROVER) optical subsystem developed by Kevin Redman. GROVER is a finite conjugate system designed to simulate the spherically-aberrated, $f/24$ HST image at the input aperture of the COS-FUV subsystem. GROVER uses the spare aspheric, conic, and turning mirrors from the optics procured for the Reflective Aberration Simulator/Calibrator (RAS/CAL), which was used for testing the Space Telescope Imaging Spectrograph and the Advanced Camera for Surveys instruments.

The aspheric mirror provides the appropriate spherical aberration into the image, while careful adjustment of the conic mirror position and tilt angles provide the correct coma and astigmatism for the desired field point. The turning mirrors were used to decrease the overall size of the system in order to fit on the CU test table and to provide the desired chief ray angle. The light source for GROVER is a sealed hollow cathode platinum lamp with a magnesium fluoride window and a single lens condenser.

Light from the GROVER optical subsystem illuminates the test optic, which then diffracts the light onto a Siegmund Scientific delay line detector with 25micron resolution in the dispersion direction. The GROVER system is placed so that it fully illuminates the test optic with the GROVER prime focus at the same distance from the grating center as the HST Cassegrain focus would be on orbit. The test optic is rotated to the nominal angle α and the detector is then located so as to be nearly tangent to the focal surface at the central β value and at the required distance from the test optic. Note that the entrance aperture and the grating surface for COS do not lie on the Rowland circle, but rather outside and inside of the nominal Rowland circle, respectively, in order to fit the instrument into the required package. The location of the test optic and the detector relative to the GROVER prime focus and optical path are initially determined

using theodolite metrology and knowledge of GROVER acquired prior to delivery of the system. Fine adjustment of the focus is accomplished by translating the grating and detector during vacuum testing. The focal plane of the detector is not curved to match the focal surface of the grating. Consequently, once the best focus is determined at one wavelength, the detector must be translated both tangent to and along the beam path in order to optimize the image for any other wavelength.

3.2. FUV Grating Efficiency Testing

The purpose of these tests is to determine the grating efficiency by measuring the efficiency of a small portion of the optic at nine points on a 3×3 grid spanning 50% of the blazed surface. Measurements are carried out at multiple wavelengths spanning the test optics nominal pass band.

The grating is illuminated by a quasi-parallel, 10mm diameter monochromatic beam at the desired test wavelength. The test detector is mounted on a rotation stage on top of a translation rail. The translation and rotation stages allow the detector to be positioned either between the test optic and the light source viewing the direct beam or close to the Wadsworth focus for the test grating viewing the diffracted beam. The translation rail is set so that it is roughly tangent to the focal surface of the Wadsworth geometry at the central β angle. The spatial response of the detector has been mapped and variations in the sensitivity are folded into the analysis. Grating tilt must be manually adjusted between vertical rows in order to ensure that the detector is properly illuminated. Care is taken to ensure that the detector is illuminated at the same angle of incidence for all measurements.

Each wavelength and position data point consists of five images: An initial incident beam, a diffracted beam image, a final incident beam image and two background images. The incident and diffracted beam images are taken in rapid succession to minimize lamp drift, and to allow an estimate of the mean brightness. If a change in brightness of greater than 5% was observed, the data set was repeated or the data point was discarded.

3.3. Grating Scatter Measurements

A set of deep images are acquired as a part of the final focal sweeps and these are co-registered for each grating the resulting deep image is carefully analyzed to determine grating scatter. By comparing the count rate in a region of the platinum spectrum known to be devoid of emission lines with all counts within the band specified in the scatter specification, an upper limit on the grating scatter can be obtained. Background subtraction is based on an unilluminated portion of the detector.

3.4. Contamination Control

Strict contamination control protocols are observed during testing to ensure that the grating efficiency or scatter characteristics are compromised by the testing process. Optics are stored in certified dry nitrogen purge when not under testing, and are never handled outside of a clean environment. We require at least a class 10,000 clean room environment for handling, and maintain our clean room at better than class 1000. We monitor for molecular contamination through the continuous use of witness plates, TQCMs and witness mirror reflectivity testing. Our greatest contamination concern is outgassing from the micropositioning stages. While these are vacuum rated, they do not meet our requirements, especially if left on for extended periods and allowed to overheat. We mitigate this outgassing by limiting the time when the stages are energized, and by venting the motors through xeloite pucks initially purchase for the FUSE program. These measures reduced the TQCM rates from 10-15Hz/hr to 4-5Hz/hr.

4. RESULTS

At the present time we have performed efficiency testing on all FUV gratings excluding the G140L Blazed, and imaging testing has been performed on all FUV gratings except for the G160M-C and G140L Blazed. All gratings for which testing has been completed have been found to be acceptable with respect to all

criteria and a full complement of flight optics has been selected. The results are summarized in figures 2 through 4 and in tables 3 and 4.

4.1. FUV Imaging and Resolution Tests

The grating imaging results were limited by the spatial resolution of the detector (estimated at 25 μ m). However, since the test detector resolution is no better than that required for the flight detector, it is reasonable to assume that achieving the resolution requirement with the test detector demonstrates adequate resolution in the grating. The results of this test are summarized in table 3, and illustrated in figure 2 for one of the test lines for G130M C.

The two values for the resolution represent the resolution determined directly from the line width (simple resolution), and from subtracting the a 0.029 arc-second equivalent width of the GROVER source (source corrected resolution). G140L C resolution values are not provided because of an error in the test setup. G160M C data has not yet been acquired. However, since both optics for each class were generated using the same test setup, it is reasonable to assume that both optics have the same imaging characteristics. Nevertheless, the flight optic in all cases is the one for which imaging data is available.

Table 3: Grating Resolution Test Results

Grating ID	Test Wavelengths	Simple Resolution $\lambda/\Delta \lambda$	Source Corrected Resolution $\lambda/\Delta \lambda$
G130M B	1219.5Å	23500	24200
	1283.7Å	22600	23100
	1382.0Å	25700	25700
G130M C	1219.5Å	23000	23700
	1283.7Å	21700	22100
	1382.0Å	22200	22600
G140L B	1219.5Å	2750	2820
	1379.0Å	2760	2820
	1524.7Å	2360	2390
G140L C	(no data)	(no data)	(no data)
G160M A	1552.3Å	19800	20200
	1621.6Å	20700	21100
G160M B	(no data)	(No Data)	(No Data)

20000112_162252_dld.fit
 GX= 0.00, GY= 0.00, GZ= 0.00
 DX= 0.00, DZ= 0.00, Gθ= 0.00

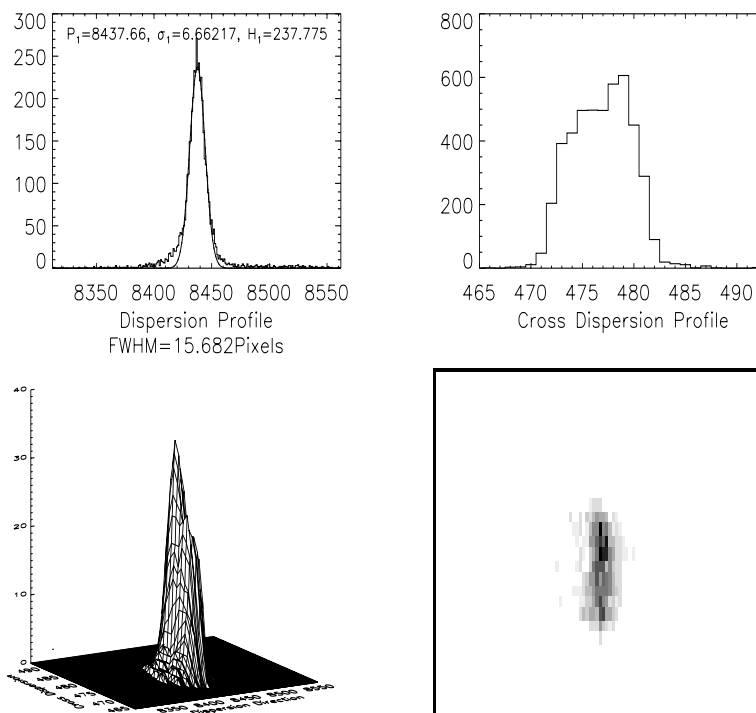


Figure 2: Sample G130M-C image of the Platinum emission line at 1283.7\AA , near the center of the G130M pass band. The pixel size is approximately $2.4\mu\text{m}$ (dispersion) by $33\mu\text{m}$ (cross dispersion). The local dispersion is $1.57\text{\AA}/\text{mm}$.

4.2. FUV Grating Efficiency

Grating efficiency measurements showed acceptable efficiency for all optics at all wavelengths and at all tested locations, for the most part being well above the minimum requirement derived from the product of the reflectivity and groove efficiency requirements. The G140L gratings proved to be very sensitive to the laminar groove profile, with the final gratings having excellent performance. In addition to the required tests, we also tested one G140L well below the specified wavelength range, and found significant efficiency, probably due to first surface reflection off of the MgF_2 coating. This suggests that there may be some possibility of operate the system below the MgF_2 cutoff if the HST telescope assembly has a similar first surface reflectivity. While these efficiencies are low, the huge collecting area of HST may provide useful throughput. Efficiency test results are summarized for all optics in figure 3.

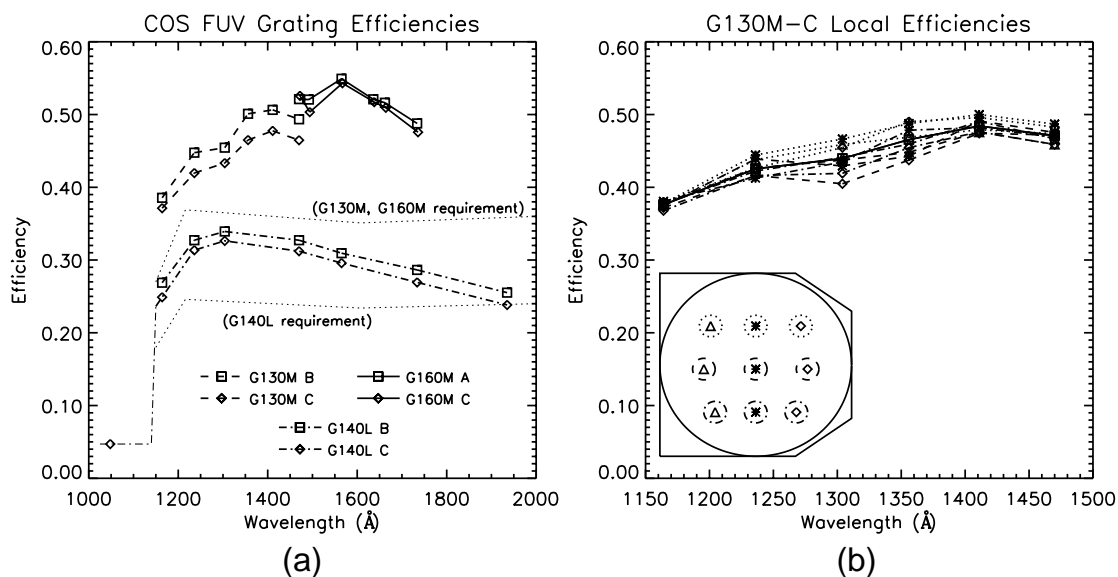


Figure 3: (a) Average grating efficiency for all delivered FUV optics compared to the requirement. Uncertainties are on the order of 2% absolute, with the dominant source being the drift in lamp output. All other contributions are on the order of 1% relative. Note that the shape of the efficiency curve shown for G140L-C between 1048Å and 1164Å is speculative. (b) Variation in efficiency versus grating position. The figure in the lower left corner illustrates the source of each data set, and the approximate size of the illuminated spot relative to the grating surface.

4.3. Grating Scatter

The grating scatter measurements indicated that the scatter is as close to the specified level as can be tested using a non-coherent source. This test can only provide an upper limit on the scatter because of the possibility that there are unidentified weak platinum lines underlying the regions selected as 'dark'. The scatter results are summarized in table 4. Figure 4 summarizes the scatter measurements for the G130M C grating.

Table 4. Grating Scatter Results

Grating ID	Measured Wavelength	Scatter
G130M B	$1209 \pm 10 \text{Å}$	$1.9 \times 10^{-5} / \text{Å}$
G130M C	$1209 \pm 10 \text{Å}$	$1.6 \times 10^{-5} / \text{Å}$
G140L B	$1140 \pm 50 \text{Å}$	$8.8 \times 10^{-6} / \text{Å}$
G140L C	$1140 \pm 50 \text{Å}$	$1.1 \times 10^{-5} / \text{Å}$
G160M A	$(\text{TBD}) \pm 10 \text{Å}$	(No data)
G160M B	$(\text{TBD}) \pm 10 \text{Å}$	(Data not reduced)

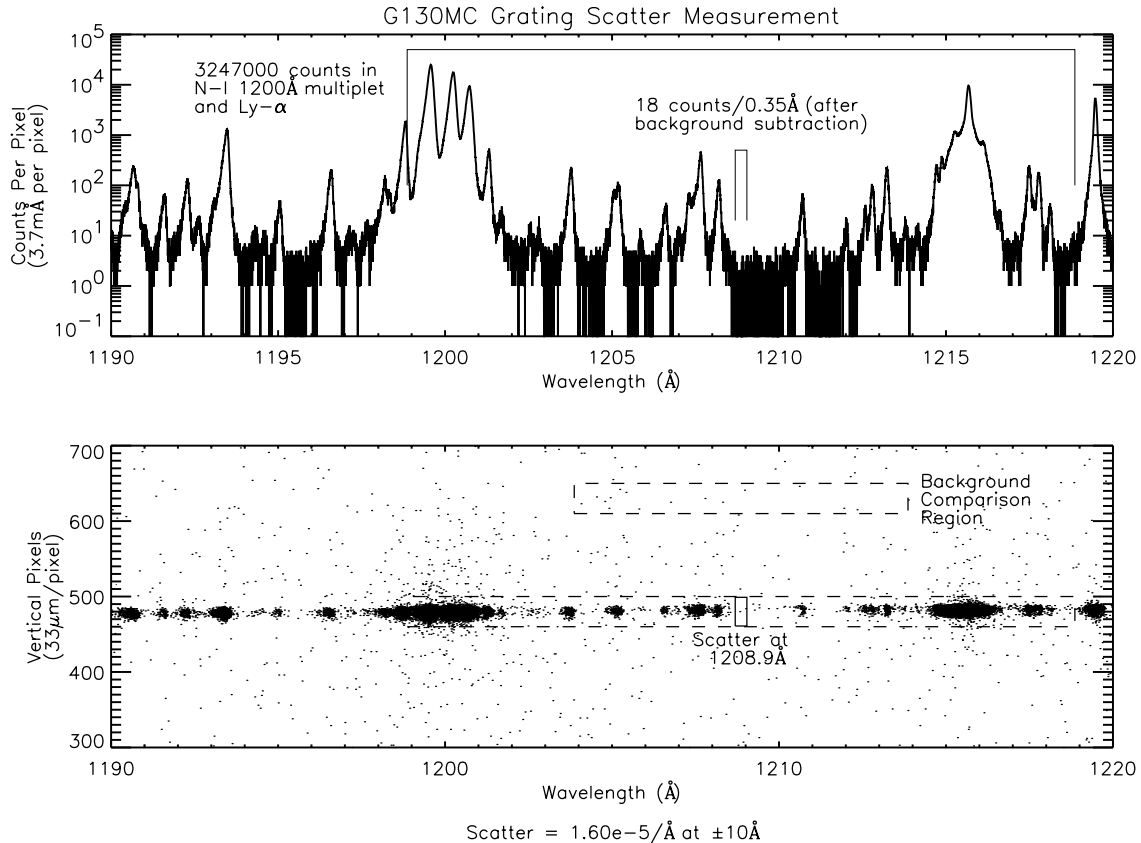


Figure 4: Grating scatter was measured to be of order $1.6 \times 10^{-5} \text{Å}^{-1}$ at $\pm 10 \text{Å}$. Because the spectrum in the selected 'dark' region is not well known, and because of the limitations imposed by counting statistics, this measurement represents an upper limit on the grating scatter. The dominant signal in this region of the spectrum is from nitrogen and hydrogen contamination of the platinum hollow cathode lamp used for the grating imaging tests. Note that this image is a composite of 22 co-registered focus images, so the resolution illustrated here is substantially below the best resolution obtained.

5. ON-ORBIT PERFORMANCE PREDICTIONS

The effective area of COS will far exceed all previous instruments due to combining the enormous collecting area of HST with excellent components in a configuration optimized for compact, dim sources (fig. 5). The effective area is simply the product of measured grating efficiency, measured detector efficiency⁶ and the estimated HST short wavelength effective area curve.⁷ The instrument collecting area quoted here exceeds initial expectations by 30 to 50%. No scale factors have been included to estimate detector efficiency decay or pre-installation optics degradation.

6. CONCLUSIONS

All of the FUV gratings for the COS program meet or exceed the mission requirements for efficiency, and one grating of each class has provided adequate imaging capacity. Flight optics have been selected from the best of the gratings delivered, and the flight spares on hand can be substituted without compromising

the mission goals. These optics, combined with the excellent detector performance and the HST collecting area, will make the Cosmic Origins Spectrograph the most sensitive medium resolution FUV spectrograph yet flown.

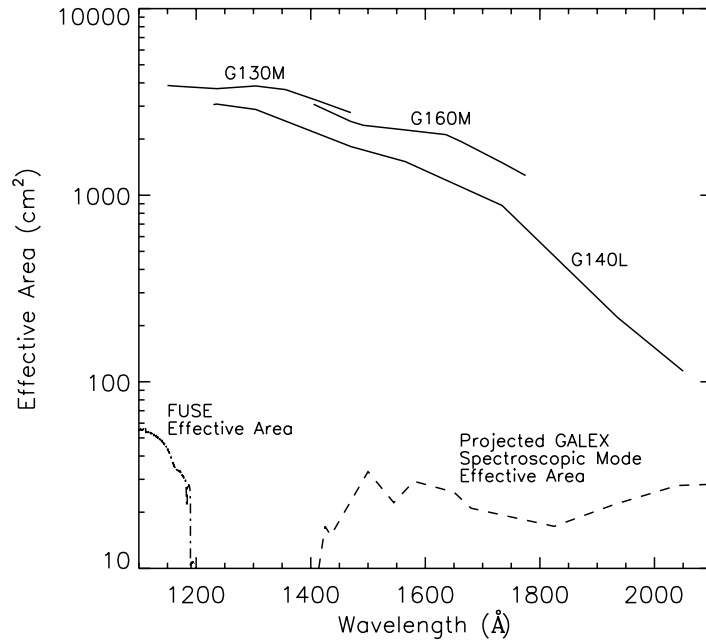


Figure 5: COS effective area based on component level test results. GALEX and FUSE effective areas are included for comparison.^{8,9}

REFERENCES

1. J. C. Green, J. A. Morse, J. Andrews, E. Wilkinson, O. H. W. Siegmund, D. Ebbets, "Performance of the Cosmic Origins Spectrograph for the Hubble Space Telescope," *Ultraviolet-Optical Space Astronomy Beyond HST, ASP Conference Series*, J. A. Morse, J. M. Shull, A. L. Kinney, **64**, pp. 176-181 (1999).
2. J. C. Green, "Cosmic Origins Spectrograph", *Proc. SPIE*, **4013** pp. 352-359 (2000).
3. O. H. W. Seigmund, "Microchannel Plate Detector Technology for Next Generation UV Instruments," *Ultraviolet-Optical Space Astronomy Beyond HST, ASP Conference Series*, J. A. Morse, J. M. Shull, A. L. Kinney, **64**, pp. 374-391 (1999).
4. S. Osterman, E. Wilkinson, G. C. Green, and K. Redman, "FUV Grating Peerformance for the Cosmic Origins Spectrograph", *Proc. SPIE*, **4013** pp. 360-366 (2000).
5. Calibration test plans and final calibration reports for each optic can be found at <http://cos-arl.colorado.edu/Documents/documents.taf>
6. John Vallerga, COS memo COS-010605-JV, 6 June 2001
7. Dennis Ebbets, Ball Aerospace & Technologies Corporation, Personal communication, July 1, 2001.
8. Dave Sahnou, Jonhs Hopkins University, Department of Physics and Astronomy, Personal communication, July 1, 2001.
9. C.D. Martin, L. Bianchi, J. Donas, T. Heckman, B. Badore, R. Malina, B. Millard, P. Friedman, M. Rich, D. Schiminovich, O. Siegmund, A. Szalay, "The Galaxy Evolution Explorer," *Ultraviolet-Optical Space Astronomy Beyond HST, ASP Conference Series*, J. A. Morse, J. M. Shull, A. L. Kinney, **64**, pp. 182-193 (1999).